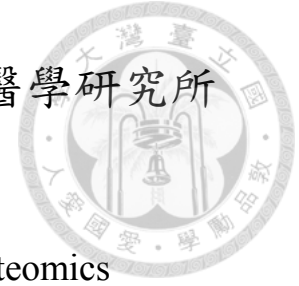


國立臺灣大學醫學院基因體暨蛋白質醫學研究所



碩士論文

Graduate Institute of Medical Genomics and Proteomics

College of Medicine

National Taiwan University

Master Thesis

亞洲特異性 ALDH2 突變造成肥胖與胰島素抵抗性的
分子機轉

Asian-specific ALDH2 mutation causes obesity and
insulin resistance: molecular mechanism

劉采晴

Cai-Cing Liu

指導教授：張以承 博士

Advisor : Yi-Cheng Chang, M.D., Ph.D.

中華民國 108 年 7 月

July 2019

國立臺灣大學碩士學位論文
口試委員會審定書

亞洲特異性 ALDH2突變造成肥胖與胰島素阻
抗性的分子機轉

Asian-specific ALDH2 mutation causes obesity and
insulin resistance: molecular mechanism

本論文係劉采晴君（學號 R06455005）在國立臺灣大學
基因體暨蛋白體醫學研究所完成之碩士學位論文，於民國
108年07月25日承下列考試委員審查通過及口試及格，特此
證明

口試委員：

張以承

（簽名）

（指導教授）

黃祥博

（簽名）

莊立民

（簽名）



所長

（簽名）



誌謝

兩年碩士生涯一晃即逝，回頭看看這一路上的歷程，心中實在有說不盡的感激。首先感謝的是我的指導教授張以承老師，老師不管是在課業或是實驗方面都提供了我很多的建議與幫助，另外也和我分享他自身的人生經歷與價值觀，也在我陷入低潮的時候給予我極大的鼓勵與安慰，我非常幸運可以在老師指導下完成我的碩士論文，這些日子真的很感謝老師的指導與教授。

另外，感謝莊立民教授在每次的實驗室會議中，對於我的進度報告提供了寶貴的意見，並鼓勵學生去進一步思考，也感謝莊立民教授與黃祥博教授在擔任口委期間針對我的論文給予建議，使論文得以更臻完善。

接著要感謝實驗室的所有同仁，謝謝蘇寧與曉薇學姊在我初進實驗室時教導我許多相關的實驗，以及當我遇到低潮的時候傾聽我的煩惱，給我關心和溫暖。謝謝孟倫學長與詩宜學姊對實驗室的付出。謝謝李博作為我論文的合作夥伴，與我一起討論實驗的設計與實作，一起找出實驗有瓶頸的部分，你的意見往往提供我在實驗上重要的線索，真的很感激能在你的協助之下完成這本論文。謝謝敬詠學姊與雅鈴在動物實驗上幫了我很多的忙，讓我能夠順利的完成實驗，也感激你們平日的照顧，總是從你們這邊收到很多關懷，讓我覺得很感動也窩心。另外也謝謝致中學弟在這段期間的幫忙，希望你能夠順利畢業。

最後我要感謝我的家人，在這忙碌的兩年當中幾乎都沒有回家，但你們還是一直默默的支持我，讓我能夠心無旁騖地專心做自己的事情，有你們的關心與打氣，讓我更有動力能在繁忙的課業中順利撐過來，希望我的努力及成長能讓你們感到欣慰及驕傲。。

最後，謹以此篇論文獻給我的師長、家人以及所有關愛我的朋友，謝謝你們。

采晴 2019.7



中文摘要

東亞地區，有過 40% 的東亞人群攜帶 *ALDH2* 特有的錯義點突變(Glu487Lys)，使其酵素在異合子酵素活性失去 60-80%，同合子酵素活性失去約 90%，此基因突變為全球盛行率最高之單一基因疾病(占~8%全球人口)。

ALDH2 (acetaldehyde dehydrogenase 2, mitochondria) 是一粒線體內的酵素，代謝乙醛為乙酸。除此之外，*ALDH2* 還會代謝多種有害醛類，包括人體的中間代謝、腸道細菌發酵、環境當中煙霧、香菸、各種塑料以及氧化壓力引發細胞脂肪過氧化而產生的有害醛類，如 4-hydroxynonenal (4-HNE)，而這些有害醛類會與蛋白質產生共價鍵修飾而改變其功能。

ALDH2 特有的錯義性點突變(Glu487Lys)在東亞人全基因組掃描中被發現與肥胖與相關表現型有關，我們以模擬人類突變的 *ALDH2* *2/*2 基因嵌入鼠為模型，發現 *ALDH2* *2/*2 基因嵌入鼠在餵食高脂高糖的飲食下，相較於對照小鼠，體重明顯上升，胰島素阻抗性增加並伴隨脂肪肝與脂肪細胞肥厚。

在這項研究中，我們探討 *ALDH2* *2/*2 基因嵌入鼠產生肥胖的原因，發現此小鼠能量消耗減少，起因推測可能與進食後產熱降低相關；另外觀察到嵌入鼠的棕色脂肪組織明顯變小。這些現象顯示此嵌入鼠可能因棕色脂肪組織功能減少、產熱降低，而產生肥胖。

我們進一步去探討分子機制，發現 4-HNE 會降低棕色脂肪細胞的脂肪酸氧化功能。利用 LC-MS/MS，我們發現 4-HNE 會與脂肪酸氧化的酵素以及電子傳遞鏈上的酵素結合，綜上所述，推測 *ALDH2* *2/*2 基因嵌入鼠會因為有害醛類累積，影響脂肪酸氧化與粒線體功能而造成小鼠肥胖。

關鍵字：乙醛脫氫酶, 醛類, 4-羥基壬烯醛, 肥胖, 能量消耗


ABSTRACT



In East Asia, approximately 40% of the East Asian population carries an inactivating missense Glu487Lys mutation of ALDH2 (SNP671) gene. The ALDH2 enzymatic activity reduces to ~60-80 % in heterozygotes and ~90 % in homozygotes of mutants. It is the most prevalent monogenetic disease in the world (~8% global population).

ALDH2 (acetaldehyde dehydrogenase 2, mitochondria) is the primary enzyme responsible for metabolizing toxic acetaldehydes in mitochondria. ALDH2 also metabolizes a variety of toxic aldehydes, including acetaldehyde from intermediate metabolism, intestinal bacterial fermentation, environmental smog, cigarette smoke, various plastics and toxic aldehydes generated from lipid peroxidation by oxidative stress, such as 4-hydroxynonenal (4-HNE). These aldehydes modify proteins by forming covalently bond crosslinks, thereby altering their biological functions.

Several recent large-scale meta-analysis of genome-wide association studies in East Asian identified ALDH2 Glu487Lys polymorphism is significantly associated with obesity and related metabolic phenotypes. In our study, we generated *Aldh2*^{*2/*2} knock-in mice mimicking the human mutation as a model. We found that *Aldh2*^{*2/*2} knock-in mice are prone to develop obesity, insulin resistance, fatty liver, and adipocyte hypertrophy on high-fat high sucrose diet as compared to controls.



We found that the *Aldh2*^{*2/*2} knock-in mice had significantly lower energy expenditure than controls. This reduction in energy expenditure may result from reduced diet-induced thermogenesis. In particular, the brown adipose tissue was markedly smaller in *Aldh2*^{*2/*2} knock-in mice. This finding suggests the reduced thermogenesis of *Aldh2*^{*2/*2} knock-in mice may result from impaired brown adipose tissue function. We further explored the molecular mechanism by which the knock-in mice have reduced brown adipose tissue function. We found 4-hydroxynonenal (4-HNE) inhibits fatty acid beta-oxidation in brown adipose tissue. Using liquid chromatography-tandem mass spectrometry (LC-MS/MS), we found that 4-HNE modifies enzymes involved in fatty acid beta-oxidation and the electron transfer chain. In summary, we found that *Aldh2*^{*2/*2} knock-in mice are prone to develop obesity, insulin resistance, and fatty liver due to reduced thermogenesis, which may be related to impaired development of brown adipose tissue and toxic aldehydes-mediated suppression of fatty acid oxidation and mitochondrial function.

Key word: ALDH2, aldehyde, 4-hydroxynonenal, obesity, energy expenditure

CONTENTS

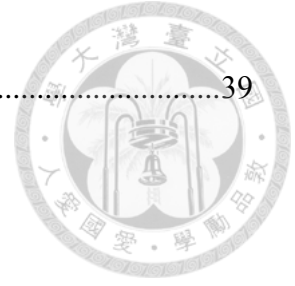


口試委員會審定書	#
誌謝	i
中文摘要	ii
ABSTRACT	iii
CONTENTS	v
Chapter I Introduction.....	1
1. Aldehyde dehydrogenase 2 (ALDH2) serves as a crucial enzyme that catalyzes aldehydes metabolism but the Glu487Lys mutation causes East-Asian specific ALDH2 deficiency	1
2. The pathogenic effects of aldehydes through form different adducts <i>in vivo</i>	2
3. Lipid peroxidation-derived products association with obesity in adipose tissue	3
4. Brown adipose tissue thermogenesis and obesity.....	4
5. Rationale of this study	6
Chapter II Materials and Methods.....	7
1. Animal model	7
2. Glucose and insulin tolerance test	7
3. Energy expenditure, food intake and physical activity.....	8



4.	Cold tolerance test and diet-induced thermogenesis test.....	8
5.	RNA extraction and RTqPCR.....	9
6.	Primary cell culture.....	10
7.	Western blot analysis	11
8.	Fatty acid oxidation assay.....	12
9.	Isolation of brown adipose tissue mitochondria	14
10.	In-solution digestion	15
11.	LC-MS/MS analysis	15
12.	Database analysis.....	16
Chapter III Result.....		17
1.	Mice with ALDH2 Glu487Lys mutation display much more obesity phenotype during High-Fat-Diet	17
2.	<i>Aldh2</i> KI mice exhibit insulin resistance and glucose intolerance	18
3.	<i>Aldh2</i> KI mice have lower energy expenditure in response to HFHSD feeding and loss the fatty acid oxidation capacity in BAT	18
4.	<i>Aldh2</i> KI mice express higher levels of modified proteins.....	21
Chapter IV Discussion.....		24
FIGURE.....		27
TABLE.....		38

REFERENCE 39



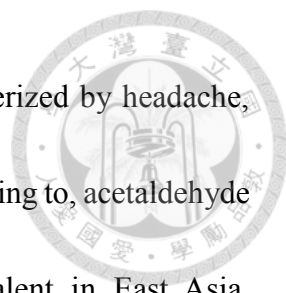
Chapter I — Introduction



1. Aldehyde dehydrogenase 2 (ALDH2) serves as a crucial enzyme that catalyzes aldehydes metabolism but the Glu487Lys mutation causes East-Asian specific ALDH2 deficiency

Aldehyde dehydrogenase 2 (ALDH2) belongs to a family of detoxifying enzymes, aldehyde dehydrogenases, (ALDHs) involved in the detoxification of aldehydes. It is located in the mitochondria and is responsible for ethanol metabolism. The pathway has two steps: ethanol is first oxidized by the alcohol dehydrogenase (ADH) in the liver to acetaldehyde. Then aldehyde dehydrogenase 2 (ALDH2) oxidizes acetaldehyde to acetate[1]. Additionally, previous reports suggest that ALDH2 shows the lowest K_m for ethanol[2, 3]. It also has the highest catalytic efficiency for acetaldehyde metabolism than other isoforms. It is estimated that, ALDH2 catalyze ~95 % acetaldehyde after ethanol intake[4, 5].

A portion of East Asian population carry a missense mutation in their *ALDH2* gene (SNPr671), which the guanine is replaced by adenine. This mutation, named the *ALDH2**2 allele, results in the substitution of lysine for glutamate in the protein at residue 487 (E487K)[6, 7]. The heterozygotes (*ALDH2* *1/*2) lost more than half the wild-type activity, and homozygotes (*ALDH2* *2/*2) only have less than 1% enzymatic activity of wild-type individuals (*ALDH2* *1/*1) [8, 9]. Individuals carries the inactive

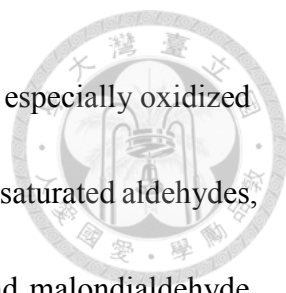


ALDH2 will develop “Asian flushing” syndrome, which is characterized by headache, facial flushing, nausea, and tachycardia after ethanol consumption owing to, acetaldehyde accumulation[10, 11]. This inactivating mutation is highly prevalent in East Asia, particularly in Southeast China, Taiwan, Japan, and Korea which is considered the most common monogenic disease across the globe (~8% global population)[12].

2. The pathogenic effects of aldehydes through form different adducts *in vivo*

ALDH2 mutation is involved in the pathogenesis of many diseases, including cardiovascular diseases, diabetes mellitus, neurodegenerative diseases, cancer, Fanconi anemia, Osteoporosis, pain, and aging[5]. These diseases are linked to aldehydes from endogenous and exogenous from the environment. Aldehydes are generated during metabolism that are intermediates or products from physiologic, biologic, and pharmacologic processes. For example, microbes produce acetaldehyde in saliva, stomach acid, and intestines. Fermented foods, alcoholic beverages, cigarette smoke, exhaust gas from automobile, factory, and various chemicals and pollutants all contain amounts of aldehydes [13, 14].

Biogenic aldehydes, primarily formed by oxidation of lipids, glucose, and primary amines, are generated from tissues with high oxidative stress. They are highly reactive electrophiles, which spontaneously react with macromolecules such as proteins, DNA,

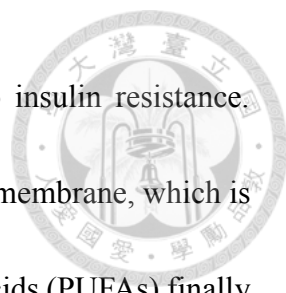


and lipids through covalent modification[15-17]. Lipid peroxidation, especially oxidized polyunsaturated fatty acids (PUFAs), leads to the generation of α,β -unsaturated aldehydes, such as 4-hydroxynonenal (HNE) and 4-hydroxyhexenal (HHE), and malondialdehyde (MDA), which are highly bioactive and are considered as “second toxic messengers”[18].

These aldehydes would react with DNA and cause genotoxic DNA modification, inhibit DNA and protein synthesis, modulate gene expression, and trigger cellular apoptosis[19, 20]. The nucleophilic side chains of histidine, cysteine, and lysine residues of protein are susceptible to the covalent attack of aldehydes. These covalent modifications result in a free carbonyl attached to the protein, termed “carbonylation”. Generation of carbonyl adducts lead to a range of pathologic damages[21-24].

3. Lipid peroxidation-derived products association with obesity in adipose tissue

In modern society, the obesity epidemic lead to a range of metabolic disorders, including fatty liver, dyslipidemia, and type 2 diabetes mellitus (T2DM)[25]. Obesity and these related metabolic disorders are associated with increased oxidative stress, lipid peroxidation, and byproducts[26-28]. The general sequence of events is that obesity induces oxidative stress level and then triggers lipid peroxidation and finally produces aldehydes by-products. However, these aldehydes can further stimulate the production of ROS that causes a vicious cycle between oxidative stress and carbonyl stress [28-30].



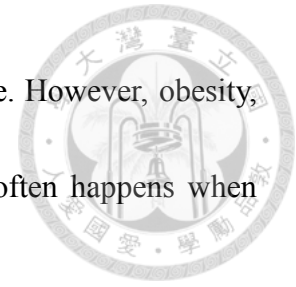
Oxidative stress induced by obesity is a major contributor to insulin resistance. Adipose tissue is rich in polyunsaturated fatty acids (PUFAs) in cell membrane, which is a target of lipid peroxidation. Peroxidation of polyunsaturated fatty acids (PUFAs) finally gives rise to the emancipation of diffusible reactive lipid aldehydes. They can diffuse into the cytoplasm and nucleus from membranes which formed in and react with a variety of proteins and DNA[22].

Among the variety reactive aldehydes, 4-hydroxynonenal(4-HNE), derived from oxidation of n-6 fatty acids, is the most reactive and cytotoxic, and most well studied [31]. For instance, mice lacking the gene mGSTA4-4 cannot catalyze HNE and are prone to develop obesity and insulin resistance[32]. On the other hand, 4-HNE was found to elevate the adipose tissue of obese humans and mice [33], and decrease insulin secretion of pancreatic islets [34, 35]. Moreover, 4-HNE also has been reported to block the insulin-signaling pathways [30, 36, 37].

4. Brown adipose tissue thermogenesis and obesity

The concept of energy homeostasis is the balance of body energy, including energy intake, energy expenditure. Energy intake means the food intake and energy expenditure consists of basal metabolic rate, the thermic effect of food (TEF), the physical activity, and the thermogenesis corresponding to the environment. When the energy intake is equal

to the energy expenditure, the energy homeostasis approaches stable. However, obesity, the well-known and significant drivers behind insulin resistance, often happens when energy intake exceeds energy expenditure [38, 39].



Brown adipose tissue plays an essential role in modulating energy expenditure, which is responsible for thermogenesis. Brown adipocytes have highly enriched uncoupling protein 1 (UCP1) located at mitochondria inner membranes, which makes protons leak across the membrane to produce heat[40]. And fatty acid β -oxidation provides fatty acid as the substrates for activating the process. The procedure of fatty acid β -oxidation is transporting the long-chain fatty acid (LCFAs) into the mitochondria matrix by the carnitine palmitoyltransferase (CPT) system, which includes CPT1, CPT2, and carnitine/acylcarnitine translocase (CACT). And acetyl-CoA is generated eventually and getting into the TCA cycle to produce ATP or uncoupling ATP production by UCP1 to produce heat. [41, 42].

Studies showed that brown adipose tissue participates in both cold-induced and diet-induced thermogenesis[43]. Inhibition of fatty acid oxidation in mice has been demonstrated severely cold intolerance[44, 45]. On the other hand, it is reported that BAT mass and activity was reduced in obese and diabetic patients[46]. BAT-mediated thermogenesis can promote energy expenditure and cope with the physiological functions and may act as a potential organ to combat obesity.

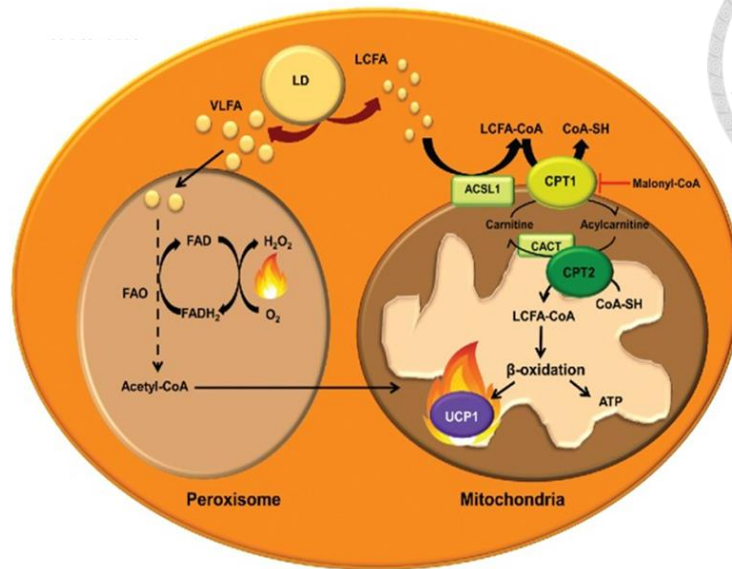


Figure 1. Brown adipocyte possesses a high capacity for fatty acid β -oxidation[42]

5. Rationale of this study

Large-scale meta-analyses of genome-wide association studies in East Asian identified *ALDH2* Glu487Lys polymorphism are associated with blood pressure, lipids, fasting plasma glucose, and body mass index[47, 48]. In our previous research also prove that *ALDH2* genetic polymorphism is associated with blood pressure and hypertension in Han Chinese[49].

Here, we utilized *Aldh2* ^{*2/*2} knock-in mice which mimic the Glu487Lys (E487K) mutation in human by homologous recombination with a C57BL/C background. We sought to determine the effects of *Aldh2* mutation on obesity and related metabolic phenotypes and explore the underlying mechanism.

Chapter II— Materials and Methods

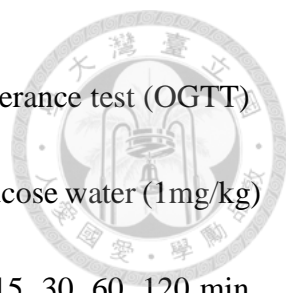


1. Animal model

Aldh2^{*2/*2} knock-in mice were provided by the Dr. Che-Hong Chen from Dr. Daria Mochly-Rosen's lab, Stanford University. *Aldh2*^{*2/*2} knock-in mice that on the C57BL/C genetic background carry the Glu487Lys (E487K) were generated by homologous recombination. All mice were housed in a temperature-controlled environment at 23°C under a 12 hr light/dark cycle. Mice were fed on high-fat-high-sucrose diet (Cat. No. D12331, Research Diets, USA) or chow diet since the age of 4 weeks, respectively. Body weight was measured weekly. All animal experiments were approved by the Institutional Animal Care and Use Committee of the Medical college of National Taiwan University.

2. Glucose and insulin tolerance test

At 24 weeks, mice were evaluated by intraperitoneal glucose tolerance test (ipGTT) after a 6-hour fasting at the age of 24 weeks. Tail blood glucose were measured at 0, 15, 30, 45, 60, 90, 120 min after intraperitoneal injection of glucose water (1mg/kg). The insulin tolerance test (ITT) were conducted at the age of 25 weeks. Briefly, mice were fasted 4 hours, and insulin (1.6IU/kg and 1.1IU/kg for HFHSD and chow diet respectively, Humulin RTM, Eli Lilly, USA) were injected intraperitoneally. Tail blood glucose were



measured at 0, 15, 30, 45, 60, 90, 120, 180 min. For oral glucose tolerance test (OGTT) conducted at the age of 26 weeks, mice were fasted for 6 hours and glucose water (1mg/kg) were given by oral gavage. Tail blood glucose was measured at 0, 15, 30, 60, 120 min following glucose administration. Acute insulin response were measured using oral glucose tolerance test (OGTT) at the age of 27 weeks. Mice blood was collected at 15 and 30 min during OGTT. Blood was centrifuged at 13000rpm, 10min, 4°C. Plasma was collected for measurement insulin concentration.

3. Energy expenditure, food intake and physical activity

Indirect calorimetry measurements were performed using the Promethion Metabolic Cage System (Promethion® , Sable Systems, Las Vegas, NV) at National Health Research Institutes Laboratory Animal Center. VO_2 and VCO_2 of individual mouse were measured for calculation of energy expenditure and the respiratory exchange ratio (RER). Wheels in the chamber was used for measurement of the distance that mice run within 24 hours. The food intake was measured for each mouse.

4. Cold tolerance test and diet-induced thermogenesis test

For a cold tolerance test, 10-week-old mice fasted for 4 hours were placed at 4°C chamber and then the rectal temperature of mice was measured at 0, 1, 2, 3, 4 hour

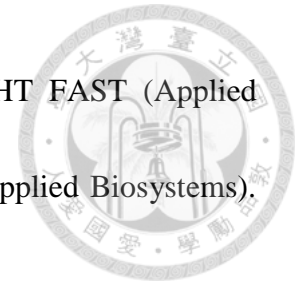
respectively. Before the diet-induced thermogenesis test, 10-week-old mice fasted overnight for 18 hours. The rectal temperature after HFHSD re-feeding were measured at 0, 15, 30, 60, 120, 180, 240 min.



5.RNA extraction and RTqPCR

Brown adipose tissue from *Aldh2* WT and KI mice was minced and harvested in 1ml of REzol C&T (Cat. No. PT-KP200CT, Protech, Taiwan). 200 μ l of chloroform was added to 1 ml of sample in Rezol, and samples were mixed vigorously by shaking for 30 seconds and then were incubated at room temperature for 5 min. Then, samples were centrifuged at 12000xg, 15min, 4 $^{\circ}$ C, and 400 μ l of the upper aqueous phase were transferred to a new 1.5 ml Eppendorf tube. An equal volume of isopropanol was added and samples were inverted several times to mix and centrifuged at 12000xg, 10 min, 4 $^{\circ}$ C. The RNA precipitate, which formed a pellet at the bottom of 1.5 ml Eppendorf tube, was washed with 75% ethanol for three times and are dried for 15 min. Pellets were dissolved the in RNase-free water. The concentration of RNA was measured by Nanodrop. cDNA were synthesized with reverse transcription kit (Cat. No. K1622, Thermo Scientific) by using the oligo(dT)18 random primer. Real-time quantitative PCR (RT-qPCR) was performed in a 10 μ l reaction with 50 ng cDNA and 0.4 μ M primer using SYBR green reagent (Cat. No. 1123ES08, YEASEN, China). Mouse Cyclophilin A mRNA was used as the internal

control. RT-qPCR reactions were performed by using ABI7900HT FAST (Applied Biosystems, USA) and Sequence Detection Systems (SDS v2.3, Applied Biosystems). All qPCR reactions were run in duplicates for each sample.



6.Primary cell culture

Brown adipose tissue from 4-6 weeks *Aldh2* WT and KI mice were minced and digested in 0.5% type I collagenase (Thermo Scientific) in 5 μ M HEPES buffer for 40 min at 37°C. The digests were centrifuged at 600g for 5 min and the supernatant was removed. The stromal vascular fraction (SVF) cell pellet was resuspended with PBS then centrifuged at 600g for 5 min. After removal of the supernatant, pellet was resuspended and cultured in 5 μ M Dulbecco's modified Eagle medium: Nutrient Mixture F-12 (DMEM/F-12) (Cat. No. 12500062, Hyclone, USA) supplemented with 10% FBS (Cat. No. 04-001-1A, Biological Industries, USA) and 1% antibiotic/antimycotic solution (Cat. No. SV30079.01, Hyclone). For differentiation, primary brown preadipocyte were exposed to induction medium containing 10% FBS, 0.5mM isobutyl-methylxanthine (Cat. no. sc-201188A, Santa Cruz Biotechnology, USA), 1 μ g/ml insulin (Humulin RTM, Eli Lilly), 5 μ M dexamethasone (Cat. no. D4902, Sigma-Aldrich, USA), 1nM T3(cat.no. T5516, Sigma-Aldrich, USA), 125 μ M indomethacin (Cat. no. I7378, Sigma-Aldrich, USA) as indicated. After 2 days, the medium was changed into DMEM/F12 containing


10% FBS, 1 μ g/ml insulin, and 1nM T3. Then we changed medium every 2 days until assay.



7. Western blot analysis

BAT homogenates from 30-week HFHSD *Aldh2* WT and KI mice were prepared using Radioimmunoprecipitation assay buffer (RIPA buffer) with protease inhibitor cocktails (cOmplete™ ULTRA Tablets, Mini, EDTA-free, EASYpack Protease Inhibitor Cocktail, Roche). The protein concentration was measured using the Bradford assay. We used 50 μ g protein on the SDS-PAGE gel and then transferred it to the polyvinylidene fluoride microporous membrane (GE Healthcare Life Science). The membranes were blocked with 10% milk in PBS containing 0,1% Tween-20, and were probed with antibodies UCP1 (Cat. no. GTX10983, GeneTex), 4HNE[HNEJ-2] (Cat. no. ab48506, Abcam), Hsp70 (Cat. no. ab45133, Abcam), GAPDH (Cat. no. MAB374, Merck). Corresponding secondary antibodies conjugated to horseradish peroxidase were used the chemiluminescence. Signal were detected using TOPBIO Chemiluminescence image system (MultiGel-21, MGIS-21-C2-6M).

The protein using for detecting with biotin hydrazide and 4HNE antibody was incubated in 10mM NaBH₄ for 30min. For carbonylated proteins, samples chemically reduced by NaBH₄ were then incubated with 5mM EZ-link biotin hydrazide (Cat. no.

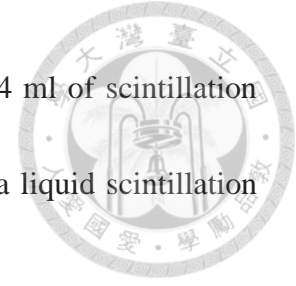


21339, Pierce) for 1 hour. After coupling, the samples are separated by SDS-PAGE gel and transferred to the polyvinylidene fluoride microporous membrane (GE Healthcare Life Science). The membrane was blocked with 10% milk in PBS containing 0,1% Tween-20 overnight at 4°C. Rinsed with PBST and incubated with Streptavidin-HRPA (Cat. no. 890803, BD Biosciences) for 1hour. Signal were detected using TOPBIO Chemiluminescence image system (MultiGel-21, MGIS-21-C2-6M).


8.Fatty acid oxidation assay

Differentiated primary brown adipocytes from *Aldh2* WT and KI mice cultured in 24-well-plate were washed with PBS three times, and incubated with 250µl palmitate/BSA buffer including 0.5 µCi [³H]-palmitate (Cat. no. PK-NET043001MC, 3H-Palmitic acid, 1mCi, PerkinElmer) for 2 hours. At the end of the incubation period, the reaction mixture was transferred to the 2ml Eppendorf tube. We then add 750µl chloroform, 250µl chloroform/methanol (1:2 volume mixture), and 250µl 2M KCl/HCl to previous 2ml Eppendorf tube in sequence. The samples were vortexed for 5 seconds and centrifuged at 3500rpm, 10min, 4°C. 600µl upper aqueous phase was transferred to new 2 ml Eppendorf tubes. 400 µl chloroform was then added and vortexed for 5 seconds, followed by addition of 400 µl methanol. Then 360 µl 2M KCl/HCl was added and vortexed for 5 seconds. The samples were centrifuged at 3500rpm, 10min, 4°C. 1ml upper

aqueous phase was transferred to scintillation vial which contains 4 ml of scintillation fluid and was measured the average counts per minute (CPM) by a liquid scintillation counter.



Regarding fatty acid oxidation of tissues, *Aldh2* KI and WT mice were fed with HFHSD for 5 weeks. Mouse BAT was isolated, weighed, and added STE buffer (0.25M Sucrose, 10mM Tris-HCl, 1mM EDTA, pH7.4), which the volume we added was 100mg/ml of tissue. BAT was homogenized using a glass Dounce homogenizer with the “Loose” pestle down and up 10 strokes each. The homogenate was poured to 1.5 ml Eppendorf tube and centrifuged at 500g for 10min at 4°C. The supernatant was decanted to new 1.5ml Eppendorf tube. We transferred 30 µl of tissue homogenate to 24-well-plate containing 370µl reaction mixture buffer which had prepared previously. Each sample was running in triplicate. The reaction mixture buffer was prepared with 100mM sucrose, 10mM Tris-HCl, 5mM KH₂PO₄, 0.2mM EDTA, 80mM KCl, 1mM MgCl₂, 2mM L-carnitine, 0.1mM malate, 0.05mM Coenzyme A, 2mM ATP, 1mM DTT, 7% BSA/5mM palmitate/ 0.01 µCi/µl [³H]-palmitate. The samples were incubated for 60min at 37°C. At the end of the incubation, the total volume of each sample was transferred to 2ml Eppendorf tube. We then add 750µl chloroform, 250µl chloroform/methanol (1:2 volume mixture), and 250µl 2M KCl/HCl in sequence. The samples were vortexed for 5 seconds and centrifuged at 3500rpm, 10min, 4°C. 600µl upper aqueous phase was transferred to



new 2 ml Eppendorf tubes. 400 μ l chloroform was then added and vortexed for 5 seconds, followed by addition of 400 μ l methanol. Then 360 μ l 2M KCl/HCl was added and vortexed for 5 seconds. The samples were centrifuged at 3500rpm, 10min, 4°C. 1ml upper aqueous phase was transferred to scintillation vial which contains 4 ml of scintillation fluid and was measured the average counts per minute (CPM) by a liquid scintillation counter.

9.Isolation of brown adipose tissue mitochondria

The BAT from 30-week-old *Aldh2* KI and WT mice were homogenized in the Dounce homogenizer with ice-cold mitochondrial isolation buffer (210mM Mannitol, 70mM sucrose, 1mM EGTA, 5mM HEPES pH7.5, 0.5%BSA), which the volume we added was 100mg/ml of tissue. The homogenate was centrifuged 800g for 10 min at 4°C and the supernatant was decanted and filtered through two-layer cheesecloth to remove residual particulates. The filtered homogenate was centrifuged by 8000g for 10 min at 4°C and carefully removed the supernatant. The pellet was resolved with 1ml mitochondrial isolation buffer and centrifuged again. The mitochondrial pellet was re-suspended in 30 μ l of STE buffer (0.25M Sucrose, 10mM Tris-HCl, 1mM EDTA, pH7.4) and protein concentration was quantitated using the Bradford assay.



10. In-solution digestion

The proteins samples in 6 M urea were reduced by 20 mM dithiothreitol for 1 h at 60°C, and alkylated by 55mM iodoacetamide for 45 min in the dark at room temperature. Then, the samples were diluted 6-fold with 50 mM triethyl ammonium bicarbonate buffer and digested with trypsin or chymotrypsin at an enzyme:protein ratio of 1:50 w/w for 16-18 h at 37 °C and 25 °C individually. Digestion was quenched by an addition of trifluoroacetic acid to a final concentration of 1%. Peptides were desalted with C18 ziptip (Millipore Corp., Billerica, MA, USA) according to the instructions of the manufacturer. Desalted and dried peptides were resuspended in 10µL of 0.1% formic acid (FA), and ready for LC-MS/MS analysis.

11. LC-MS/MS analysis

LC-MS/MS analysis was performed on a NanoACQUITY UPLC System (Waters, USA) coupled to a high-resolution mass spectrometer (QE HF-X, Thermo Fisher Scientific, USA). The peptides were injected into a trap column (2 cm × 75 µm i.d., Symmetry C18), then separated in a 25 cm × 75 µm i.d. BEH130 C18 column (Waters, USA) by a gradient from 0% to 85% buffer B (buffer A, 0.1% formic acid in H₂O; buffer B, 0.1% formic acid in acetonitrile). The mass spectrometer is operated in data-dependent mode with the following acquisition cycle: a MS scan (m/z 350–1600) recorded at

resolution $R = 60,000$; MS/MS scans recorded at resolution $R = 15,000$, which are acquired by HCD fragmentation with collision energy of 28.



12. Database analysis

MS/MS spectra were searched with the Mascot engine (v2.6, Matrix Science, UK) against the UniProtKB mouse protein database using the following parameters: the mass tolerance of precursor peptide was set as 20 ppm, and the tolerance for MS/MS fragments was 0.02 Da with maximum two missed cleavage. The modifications of peptides were set as follows: static carbamidomethylation on cysteine, variable oxidation on methionine, variable deamidation of asparagine or glutamine, and variable 4-HNE modification on cysteine, histidine and lysine. The cut-off threshold of significant peptide-to-spectrum matches is $p < 0.05$.

Mitochondrial modified proteins biological function were confirmed by using the Uniport database. Then we used g:Profiler to get the “Kyoto Encyclopedia of Genes and Genomes (KEGG) pathways” and “Gene ontology biological process” information.


Chapter III— Results



1. Mice with ALDH2 Glu487Lys mutation display much more obesity phenotype during High-Fat-Diet

To assess the effect of ALDH2 Glu487Lys mutation on obesity, we placed wild-type mice and *Aldh2* *2/*2 knock-in mice (herein *Aldh2* WT mice and *Aldh2* KI mice) on a regular chow diet or high-fat high-sucrose diet (HFHSD) for 16 weeks. *Aldh2* KI mice exhibited a significant weight gain compared to *Aldh2* WT mice (Figure 1A). Body composition analyses showed that *Aldh2* KI mice have significantly higher fat mass, lean mass and total water (Figure 1B). However, *Aldh2* KI mice fed with a chow diet for 16 weeks did not exhibit differences in body weight and body composition (Figure 2A and 2B). *Aldh2* KI mice had a significant increase in each depot of white adipose tissue, including inguinal and perigonadal fat. Conversely, the brown adipose tissue is significantly smaller in *Aldh2* KI mice (Figure 2C). Compared with *Aldh2* WT mice, *Aldh2* KI mice had significantly larger adipocyte size but similar adipocyte number in perigonadal white adipose tissue (Figure 2D). Besides, HFHSD-fed *Aldh2* KI mice had higher mass and hepatic triglycerides content of the liver and developed severe hepatic steatosis (Figure 2E and 2F).

2. *Aldh2* *2/*2 knock-in mice exhibit insulin resistance and glucose intolerance

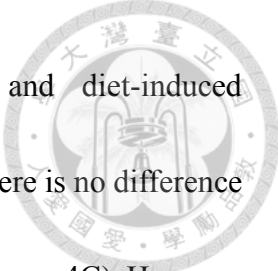


Aldh2 KI mice have worsened glucose tolerance than *Aldh2* WT mice during intraperitoneal glucose tolerance test (ipGTT) (Figure 3A). Insulin tolerance test (ITT) showed impaired insulin sensitivity in HFHSD-fed *Aldh2* KI mice (Figure 3B). Consistently, the oral glucose tolerance test (OGTT) demonstrated the same trend. *Aldh2* KI mice also exhibited compensatory increase in acute insulin secretion (Figure 3C and 3D). However, there was no difference between *Aldh2* KI mice and WT mice on the chow diet (Figure 3).

These data show East-Asian-specific *Aldh2* mutation causes obesity, hepatic steatosis, insulin resistance, and glucose intolerance in mice on HFHSD.

3. *Aldh2* *2/*2 knock-in mice have lower energy expenditure in response to HFHSD feeding and loss the fatty acid oxidation capacity in BAT


To explore the mechanism by which *Aldh2* KI mice are prone to develop obesity and related metabolic phenotypes, we measured their energy balance including energy intake and expenditure. Indirect calorimetry showed that *Aldh2* KI mice exhibit lower oxygen consumption and energy expenditure at dark phase (Figure 4A). The basal metabolic rate is similar between *Aldh2* KI mice and WT mice. There is also no change in food intake and physical activity between two strains (Figure 4B). We next examine



thermogenesis function including cold-induced thermogenesis and diet-induced thermogenesis. When mice were placed at a 4°C cold environment, there is no difference of temperature change between *Aldh2* KI mice and *Aldh2* WT mice (Figure 4C). However, *Aldh2* KI mice exhibited significantly lower diet-induced thermogenesis (DIT), defined as the thermogenesis food ingestion (Figure 4D). These data suggest that reduced diet-induced thermogenesis in *Aldh2* KI mice might be a major cause of decreased energy expenditure.

We next investigated the causes of reduced thermogenesis in *Aldh2* KI mice. Brown adipose tissue plays a vital role in adaptive thermogenesis and its unique protein, uncoupling protein-1 (UCP1), generates heat by uncoupling oxidative phosphorylation. [40]. For this process, fatty acid β -oxidation is essential and provides substrates for uncoupling in BAT[50, 51]. And it has been showed that thermogenic brown adipocyte possesses a high capacity for fatty acid β -oxidation. Chondronikola et al. also reported that BAT mitochondrial thermogenesis is 45-fold greater than that of white adipose tissue. [52]. Thus, we hypothesized the reduced thermogenesis and energy expenditure of *Aldh2* KI mice are probably due to reduced brown adipose tissue mass.

To understand the function of fatty acid β -oxidation, we measured the fatty acid β -oxidation related genes and thermogenic gene in brown adipose tissue from *Aldh2* KI and WT mice fed HFHSD. *Aldh2* KI BAT showed a significantly reduced expression of fatty



acid β -oxidation-related genes, including *Cpt1b*, *Cpt2*, and *Aco1*. On the other hand, there is no difference in the expression of *UCP1* (Figure 5A and 5B). Since previous studies showed that aldehydes accumulate in *Aldh2* KI mice, we evaluated the effect aldehydes on the function of brown adipose tissue. Primary brown preadipocytes were isolated from 4-week-old mice and induced into mature brown adipocytes. We found that 4-HNE inhibited fatty acid oxidation in a concentration-dependent manner (Figure 5C). Furthermore, primary brown adipocytes isolated from *Aldh2* KI mice showed a significant decrease of fatty acid oxidation as compared to *Aldh2* WT mice (Figure 5D).

Following this finding, we further investigated the fatty acid oxidation capacity of whole brown adipose tissue. *Aldh2* KI mice and WT mice were fed HFHSD for five weeks, and fresh BAT was isolated for fatty acid oxidation assay. There is a non-significant reduction in fatty acid oxidation capacity of whole brown adipose tissue of *Aldh2* KI mice. These data show that the decrease fatty acid β -oxidation of BAT in *Aldh2* KI mice may explain the decreased energy expenditure observed in *Aldh2* KI mice.

4. *Aldh2* ^{*2/*2} mice express higher levels of modified proteins

ALDH2 mutation is characterized by the inactive ALDH2 enzyme activity, which fails to metabolize toxic aldehydes. As a result, these bio-reactive aldehydes, such as 4HNE, will attack proteins and alter their functions. To examine the hypothesis, we explored the extent of 4HNE-adduction and protein carbonylation in the *Aldh2* KI and WT mice.

Based on previous research, 4HNE modified proteins has been extensively studied and involved in the development of a variety of metabolic diseases[53-55]. However, the protein modification by 4HNE in brown adipose tissue is still unclear. Chronic dietary nutrient overload accelerated obesity and is associated with enhanced mitochondria oxidative stress, increasing lipid peroxidation in adipose tissue[56]. The brown adipose tissue has a large capacity for mitochondria fatty acid β -oxidation, which is critical for regulating energy balance. Loss of the brown adipose tissue mitochondria fatty acid oxidation function due to modification by aldehyde adduction may result in energy imbalance in *Aldh2* KI mice.

We first compared the pattern of 4-HNE modified proteins and carbonylation proteins of BAT from *Aldh2* KI and WT mice using 4HNE antibody and biotin hydrazide-tagged aldehyde reactive probe, respectively. Western blot showed increased levels of carbonylation proteins (left panel) and 4-HNE adducted protein (right panel) in *Aldh2* KI

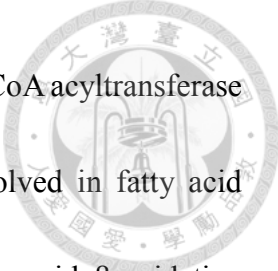


mice as compared to controls (Figure 6A).

The workflow presented an analytical scheme for identifying the 4-HNE-modified proteins in the *Aldh2* KI and WT mice at the age of 30 weeks. *Aldh2* KI and WT mice were fed HFHSD and the brown adipose tissue mitochondrial proteins were isolated. Proteins were digested with trypsin and subjected to liquid chromatography-tandem mass spectrometry (LC-MS/MS). Then the MS data were queried by the Mascot software (Figure 6B).

We used 2 *Aldh2* KI and 2 WT mice in the study. After removing all the proteins that were detected without 4HNE modified, a list of soluble proteins considered as targets of 4HNE modification in BAT were generated (Table1). A total of 20 proteins were identified, and ten mutual proteins were showed between *Aldh2* KI and WT mice. And it revealed that *Aldh2* KI mice have more modified proteins than *Aldh2* WT mice (Figure 6C and 6D).

We used online bioinformatics resources g:Profiler to obtain the Kyoto Gene Encyclopedia and genomic pathway (KEGG pathway) and Gene ontology biological process to assess the association of these proteins. Protein functional information were provided from the Uniprot database. Some of proteins are associated with mainly metabolic processes, including fatty acid, amino acid, and nucleotide metabolism and TCA cycle and others are related to oxidative phosphorylation, respiratory electron



transport chain, NADH and ATP metabolic process (Table 1). Acetyl-CoA acyltransferase 2 (*Acaa2*), one mutual protein in *Aldh2* WT and KI mice, is involved in fatty acid metabolism. And it is also the last step of the mitochondrial fatty acid β -oxidation pathway by breaking down fatty acid into acetyl-CoA. On the other hand, proteins are involved in energy metabolism, such as NADH dehydrogenase [ubiquinone] 1 subunit C2 (*Ndufc2*), cytochrome b-c1 complex subunit 7 (*Uqcrb*) and so on.

Chapter IV— Discussion



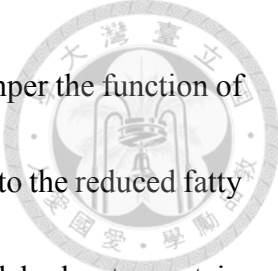
In this study, we found that *Aldh2* knock-in mice mimicking the East-Asian-specific ALDH2 Glu487Lys mutation are prone to develop obesity, fatty liver, insulin resistance and glucose intolerance. The obesity phenotype is probably caused by reduced energy expenditure and thermogenesis. Unexpectedly, we observe that the brown adipose tissue is remarkably smaller in *Aldh2* KI mice compared to wild-type mice, either on chow diet or HFHSD. We further found the fatty acid oxidation capacity is reduced in BAT of *Aldh2* KI mice, which may lead to the observed reduced thermogenesis.

Brown adipose tissue generates heat primarily within the mitochondria through fatty acid oxidation and uncoupling of oxidative phosphorylation mediated by UCP1. The fatty acid can be activators of the UCP1 for thermogenesis or be suppliers in the electron transport chain for generating ATP. The oxidation of fatty acid in brown adipocyte represents a major source of thermogenesis[57]. Suppression of fatty acid oxidation compromise thermogenesis. For instance, adipose-specific knockout *CPT2* mice presented the hypothermic when they were exposed in a cold environment. And the thermogenic genes in *CPT2* mice brown adipose tissue didn't up-regulate under the agonist-induced stimulation[45, 58]. When ACSL1, an enzyme catalyzing the formation of acyl-CoA that are used for β -oxidation, are impaired in adipose tissue. The *Acs11^{A-/-}* mice are also showed cold intolerance due to impaired fatty acid oxidation[44]. It

indicates that mitochondrial fatty acid β -oxidation is critical for the thermogenesis.

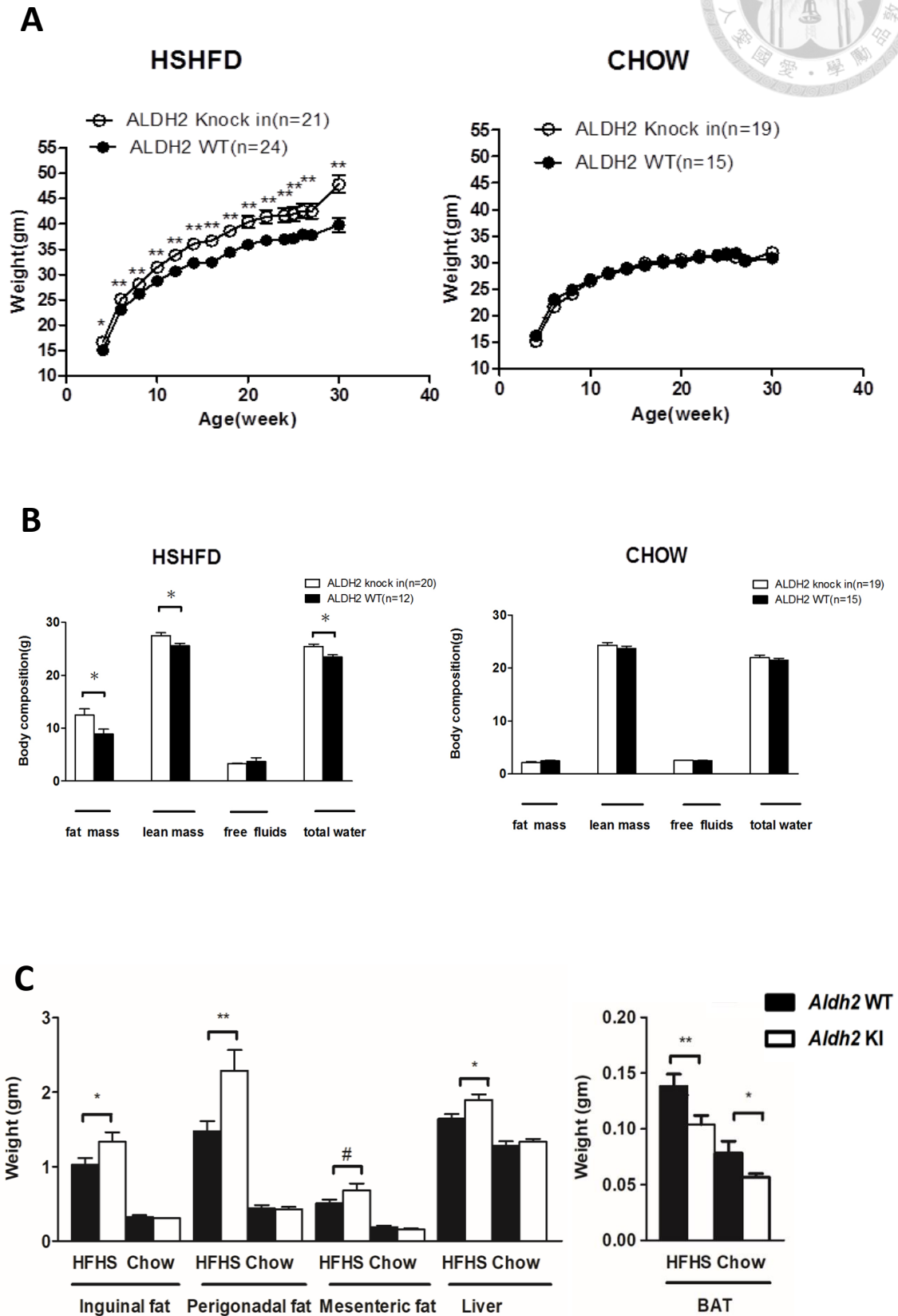
In this study, we did not observe altered UCP1 expression in *Aldh2* knock-in mice. However, either primary brown adipocytes or whole brown adipose tissue isolated from *Aldh2* KI mice exhibited reduced fatty acid oxidation capacity. We hypothesize it may link to the higher aldehyde production in the BAT mitochondria of *Aldh2* KI mice. Indeed, we observed that either 4-HNE-modified proteins or carbonylated proteins are enriched in the BAT isolated from *Aldh2* KI mice.

Using LC-MS/MS, we further demonstrated that 4-HNE conjugated to the proteins involved in mitochondrial electron transfer chain and fatty acid oxidation. And these proteins demonstrated higher amount in *Aldh2* KI mice. The conjugation of 4-HNE to these proteins may interfere fatty acid oxidation. Consistent with our finding, mitochondrial dysfunction caused by oxidative stress and the ROS-initiated lipid peroxidation byproducts has been reported to be involved a range of disease in recent years[59, 60]. And it also indicates about 30% of 4-HNE-modified proteins formed in cell existing in mitochondria and is considered as the major candidate to cause mitochondrial dysfunction[61, 62]. Previous studies have demonstrated the 4-HNE modified proteins plays important role in the pathogenesis of Alzheimer's disease[63, 64], rheumatological diseases and other autoimmune disease[65], gastrointestinal diseases[66], myocardial diseases[67], and cancer[68, 69].



Our study supports that 4-HNE or other toxic aldehydes may dampen the function of BAT, leading to obesity and related metabolic phenotypes. In addition to the reduced fatty acid oxidation, which is probably caused by the adduction of aldehydes to protein involved in fatty acid oxidation and mitochondrial electron transfer chain, we also observe that the BAT of *Aldh2* KI mice is much smaller in volume than wild-type controls. The underlying mechanism is currently unknown. It may be related to the impaired embryonic development of BAT. Therefore, we are currently investigating the embryonic development of BAT in *Aldh2* KI and WT mice.

FIGURE



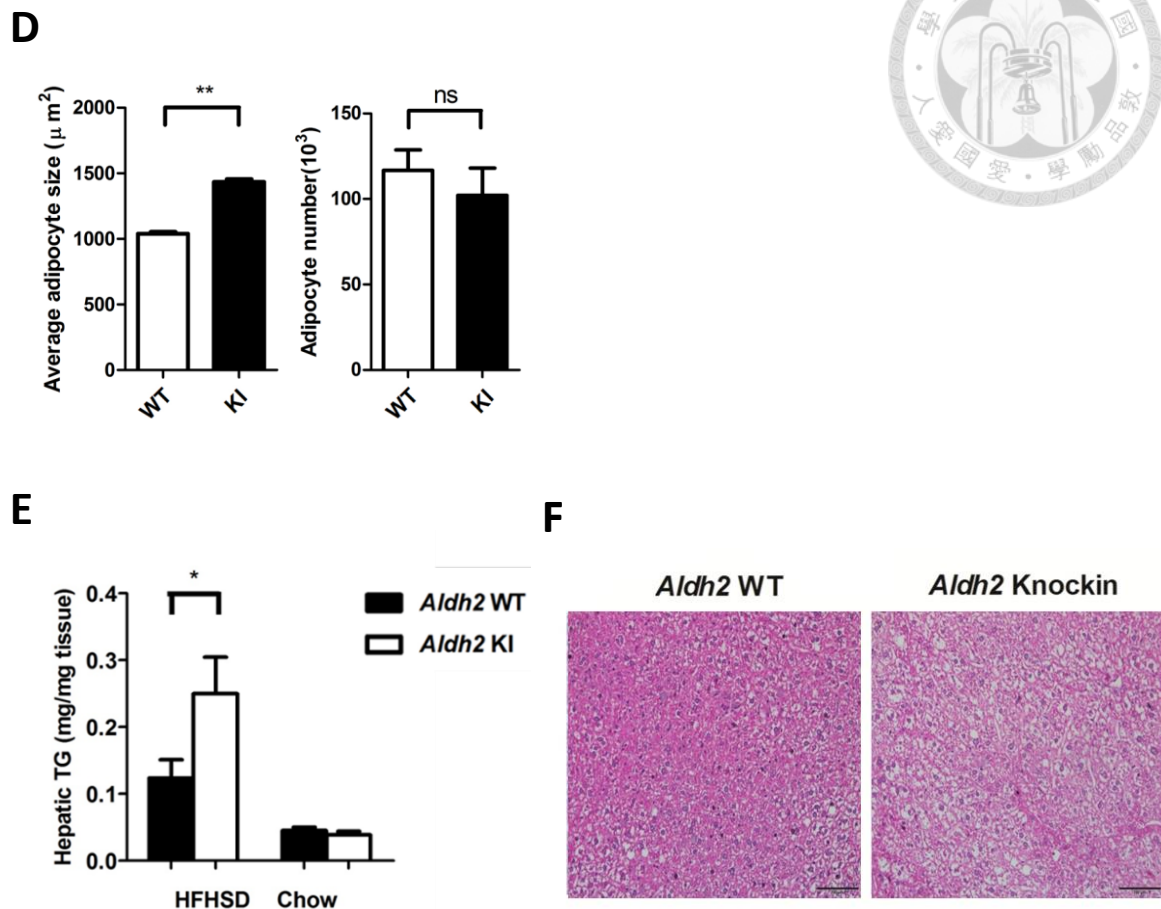


Figure 2. Phenotype of *Aldh2* $*2/*2$ knock-in mice and wild-type mice

(A) Body weight on HFHSD (n=21:24) and chow diet (n=19:15)

(B) Body composition on HFHSD (n=20:12) and chow diet(n=19:15)

(C) Distribution tissue weight of inguinal fat (subcutaneous), perigonadal fat

(intraabdominal fat), liver, and brown adipose (BAT) of *Aldh2* $*2/*2$ knock-in mice

(KI) and wild-type (WT) mice on HFHSD(n=78:67) or chow diet (n=12:10)

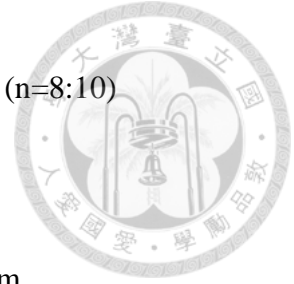
(D) Perigonadal fat adipocyte size and number from *Aldh2* $*2/*2$ knock-in mice (KI)

and wild-type (WT) mice fed HFHSD (n=17:24)

(E) Hepatic triglyceride content of HFHSD (n=23:20) and chow diet (n=8:10)

(F) Representative H&E stain of liver

* P < 0.05, ** P < 0.01, ***P<0.001. Data presented as mean \pm s.e.m.



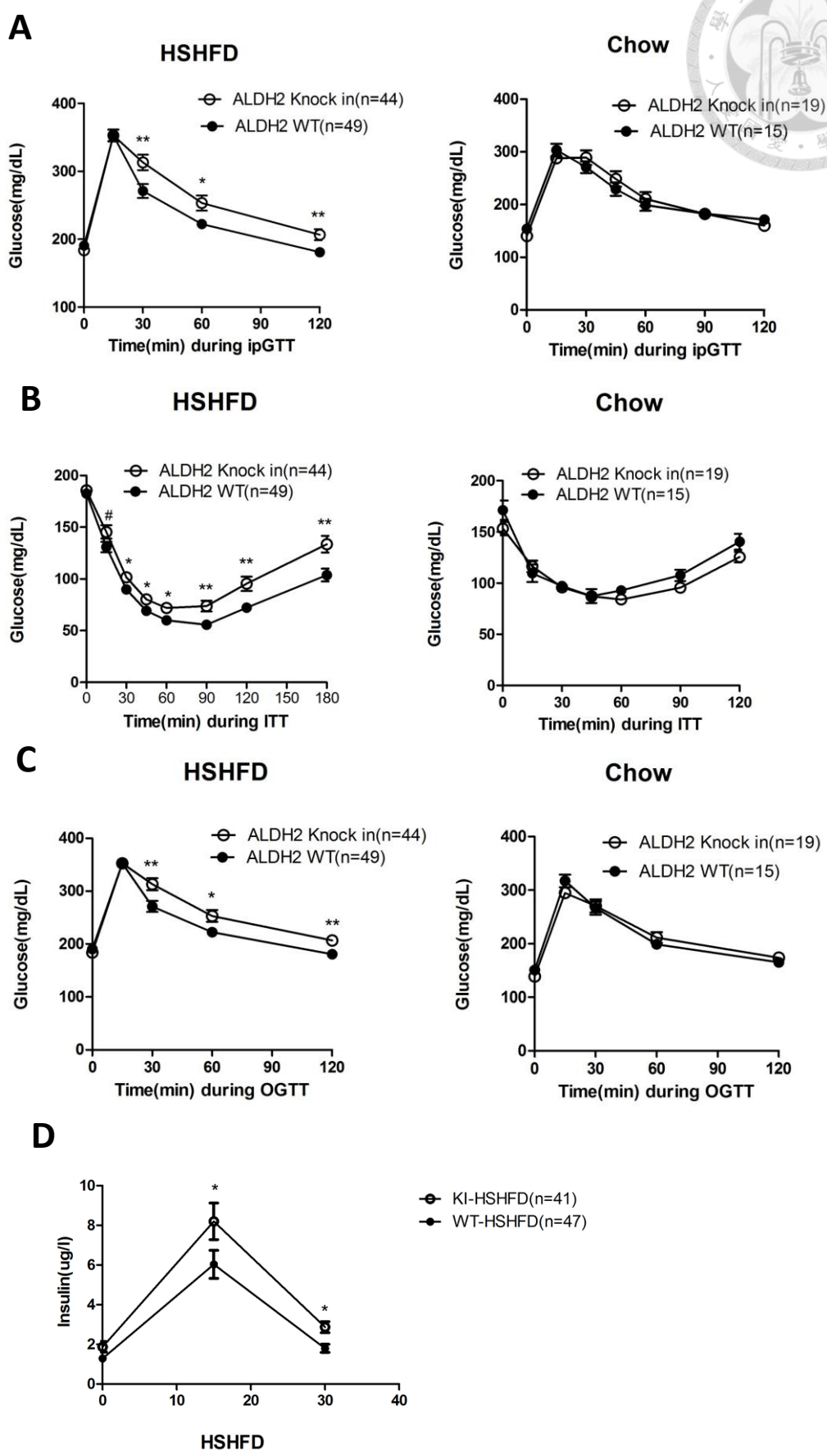
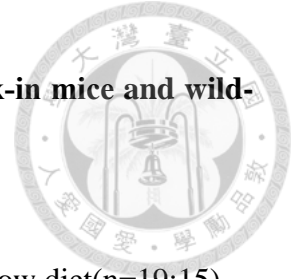


Figure3. Glucose and insulin tolerance test of *Aldh2* *2/*2 knock-in mice and wild-type mice



(A) Intraperitoneal glucose tolerance test on HFHSD(n=44:49) or chow diet(n=19:15)

(B) Insulin sensitivity test on HFHSD(n=44:49) or chow diet(n=19:15)

(C) oral glucose tolerance on HFHSD(n=44:49) or chow diet(n=19:15)

(D) insulin response during OGTT on HFHSD(n=41:47)

* P < 0.05, ** P < 0.01, ***P<0.001. Data presented as mean \pm s.e.m.

ipGTT: Intraperitoneal glucose tolerance ;OGTT: oral glucose tolerance; ITT: insulin tolerance test

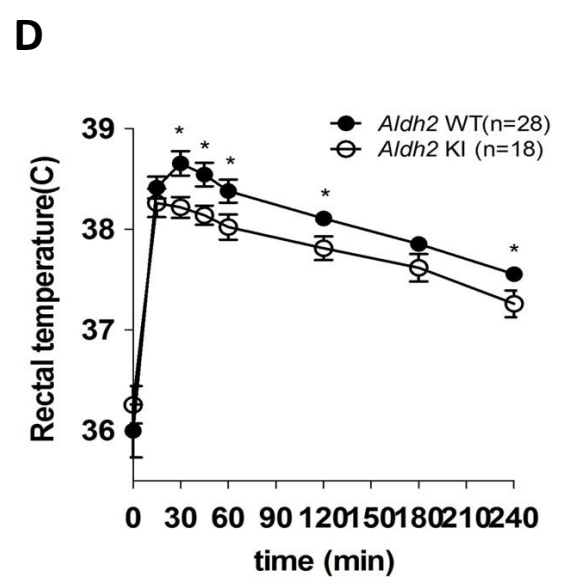
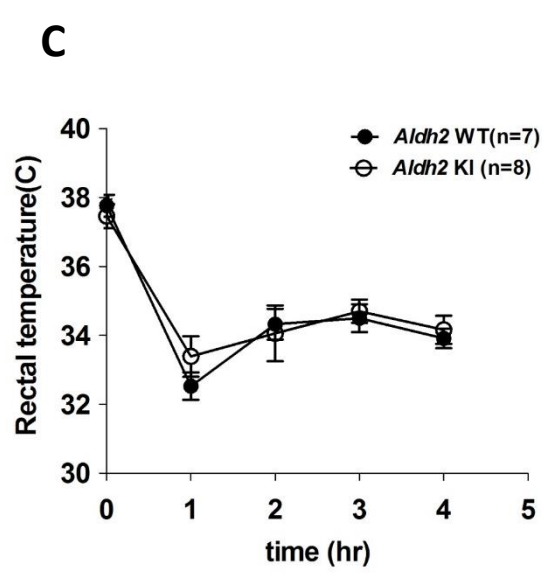
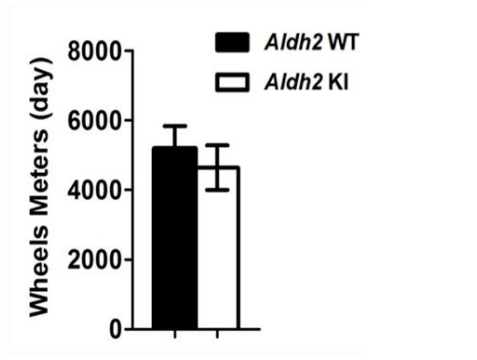
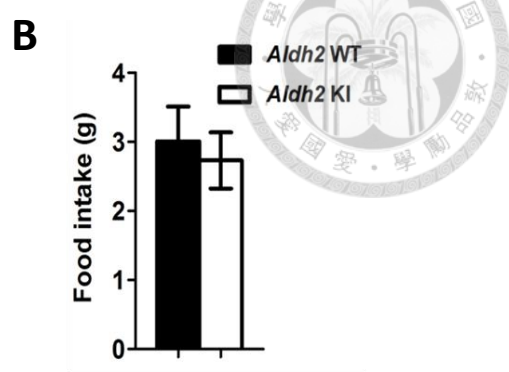
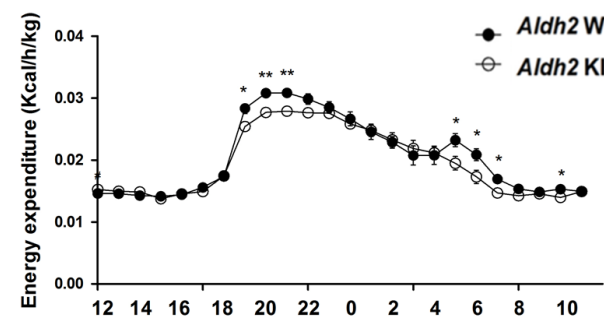
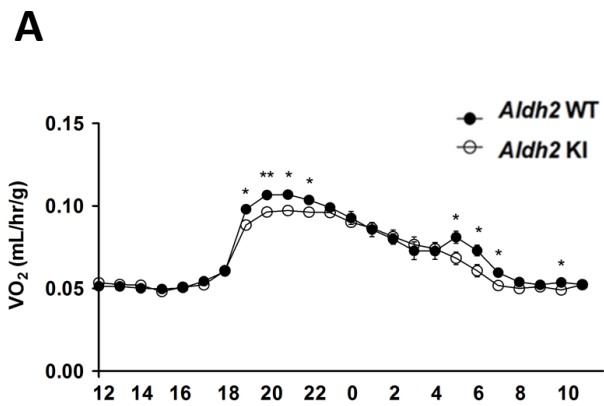




Figure4. *Aldh2*^{*2/*2} knock-in mice decrease energy expenditure in response to

HFHSD

(A) Relative oxygen consumption (VO₂) and energy expenditure over a 24-hr period

(n=12:12)

(B) Metabolic parameters of food intake and wheel meters (n=12:12)

(C) The temperature of cold-induced thermogenesis (n=7:8)

(D) The temperature of diet-induced thermogenesis (n=8:8)

* P < 0.05, ** P < 0.01, ***P<0.001. Data presented as mean ± s.e.m.

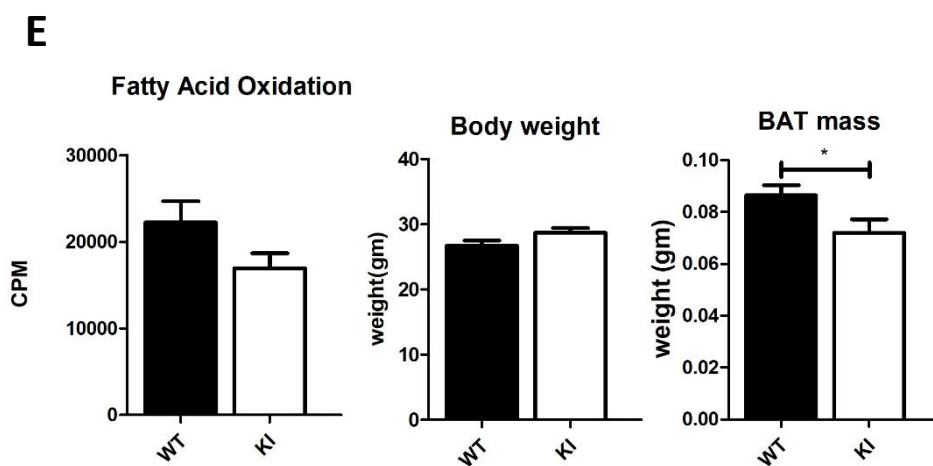
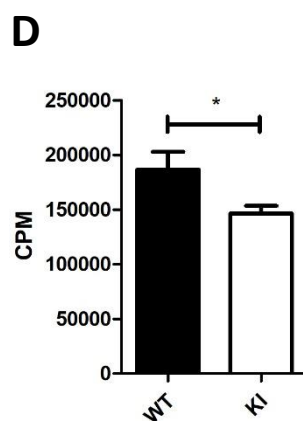
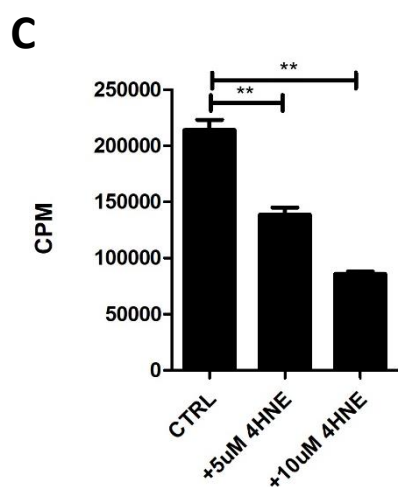
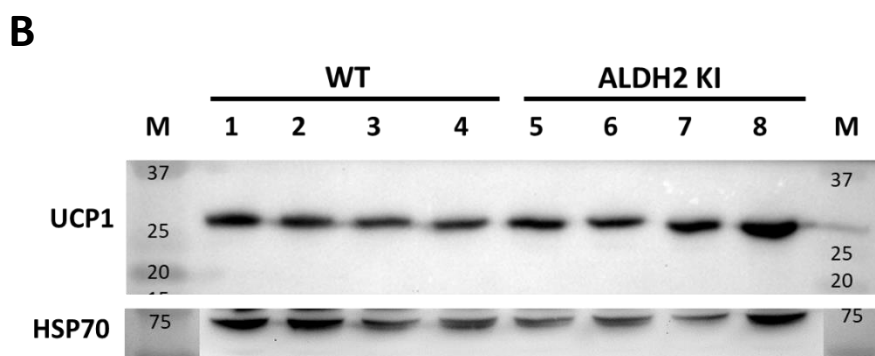
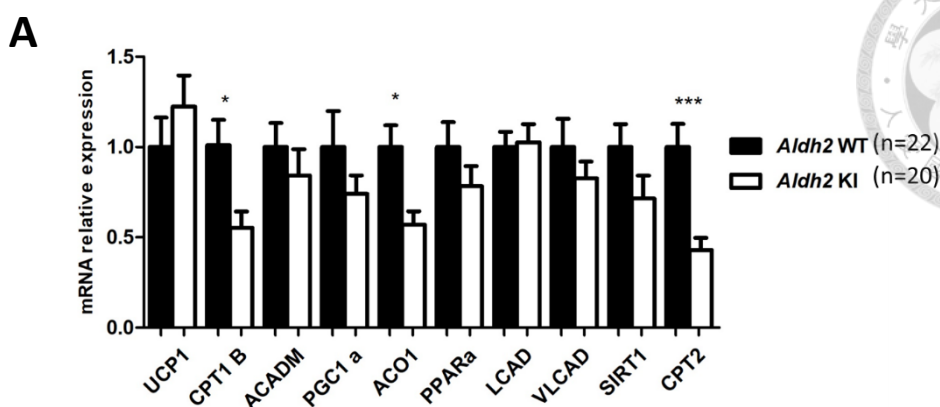




Figure 5. The effect of impaired ALDH2 activity inhibits fatty acid oxidation in brown adipose tissue

(A) Quantitative real-time polymerase chain reaction(qPCR) analysis of mRNA for fatty acid oxidation and thermogenic genes in BAT (n=22:20)

(B) Western blot of UCP1 in BAT of *Aldh2* *2/*2 knock-in mice and wild-type mice fed HFHSD (n=4:4)

(C) Fatty acid oxidation was measured in primary brown adipocytes which treated different 4HNE concentration

(D) Fatty acid oxidation was measured in primary brown adipocytes from *Aldh2* *2/*2 knock-in and wild-type mice (n=15:15)

(E) Fatty acid oxidation was measured with BAT from *Aldh2* *2/*2 knock-in and wild-type mice fed 5week HFHSD. The body weight and BAT mass were measured(n=14:10)

* P < 0.05, ** P < 0.01, ***P<0.001. Data presented as mean \pm s.e.m.

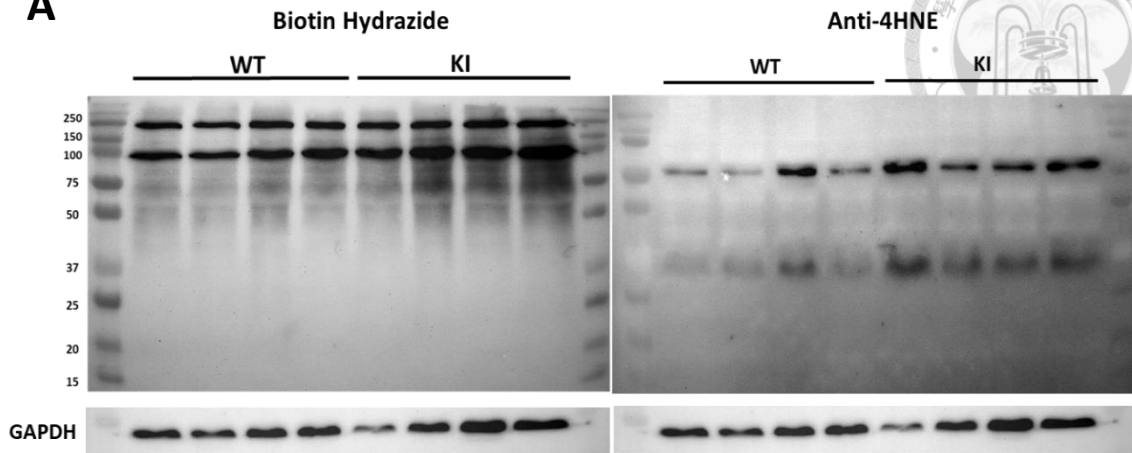
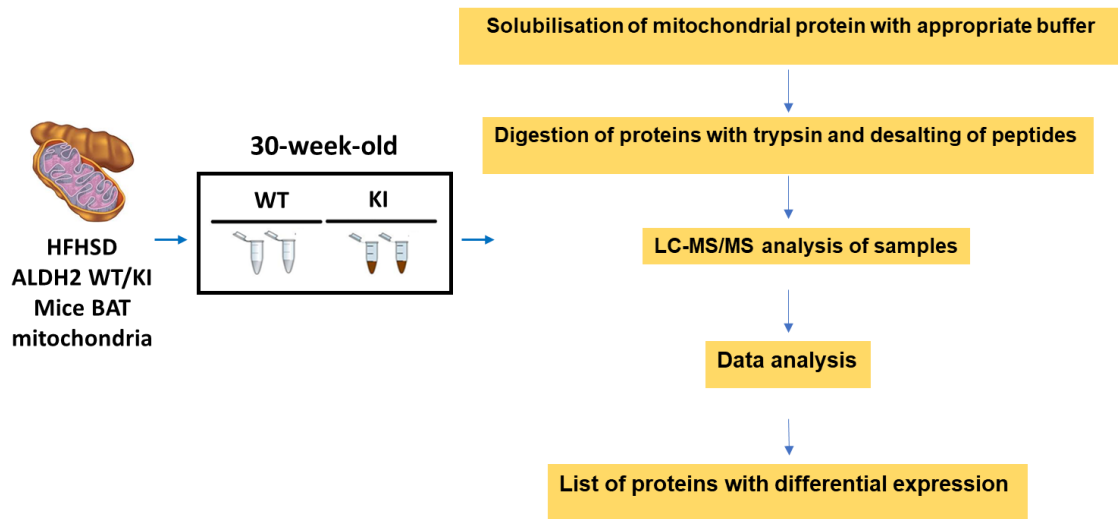
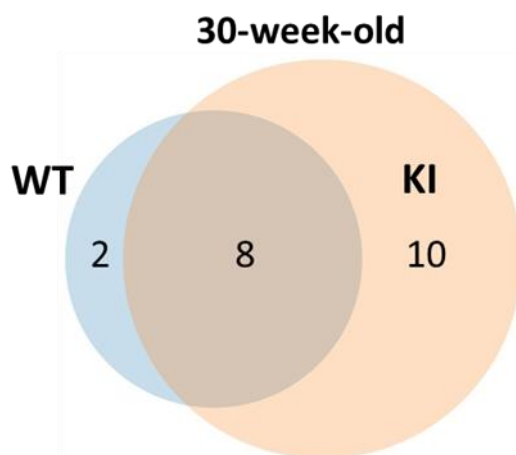
A**B****C**

Figure 6. LC-MS/MS Analysis the BAT mitochondrial modified protein by 4HNE



(A) Detection of carbonylated proteins and 4-HNE modified proteins in BAT from *Aldh2*

**2/*2* knock-in mice and wild-type mice fed HFHSD (n=4:4)

(B) Experimental design and workflows used in the study

(C) Comparison of identified proteins from *Aldh2* **2/*2* knock-in mice and wild-type

mice at the age of 30 weeks

(D) Venn diagram of identified proteins from *Aldh2* **2/*2* knock-in mice and wild-type

mice

TABLE

Table1. 4HNE modified protein list of 30-week-old mice fed HFHSD

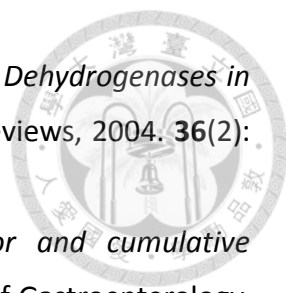


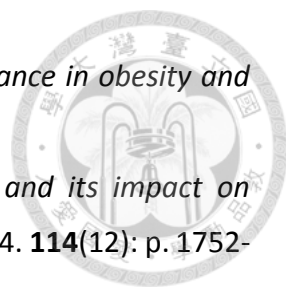
WT			
Gene name	Uniprot ID	protein name	biological function
Acaa2	Q8BWT1	3-ketoacyl-CoA thiolase, mitochondrial	fatty acid beta-oxidation
Atp5f1a	Q03265	ATP synthase subunit alpha, mitochondrial	ATP biosynthetic process
Immt	Q8CAQ8	MICOS complex subunit Mic60	maintenance of mitochondrial architecture
Immt	E9Q800	MICOS complex subunit MIC60(isoform)	maintenance of mitochondrial architecture
Uqcrb	Q9CQB4	Cytochrome b-c1 complex subunit 7	mitochondrial electron transport
Uqcrl1	Q9CR68	Cytochrome b-c1 complex subunit Rieske, mitochondrial	mitochondrial electron transport
Hspa8	P63017	Heat shock cognate 71 kDa protein	MAPK signaling pathway
Uqcrl1	A0A0A6YVZ0	Cytochrome b-c1 complex subunit 1, mitochondrial	mitochondrial electron transport
Atp5a1	D3Z6F5	ATP synthase subunit alpha	ATP synthesis coupled proton transport
Chchd3	D3Z0L4	MICOS complex subunit	maintenance of mitochondrial architecture
KI			
Gene name	Uniprot ID	protein name	biological function
Atp5f1a	Q03265	ATP synthase subunit alpha, mitochondrial	mitochondrial electron transport
Immt	Q8CAQ8	MICOS complex subunit Mic60	maintenance of mitochondrial architecture
Immt	E9Q800	MICOS complex subunit MIC60(isoform)	maintenance of mitochondrial architecture
Uqcrb	Q9CQB4	Cytochrome b-c1 complex subunit 7	mitochondrial electron transport
Uqcrl1	Q9CR68	Cytochrome b-c1 complex subunit Rieske, mitochondrial	mitochondrial electron transport
Hspa8	P63017	Heat shock cognate 71 kDa protein	MAPK signaling pathway
Uqcrl1	A0A0A6YVZ0	Cytochrome b-c1 complex subunit 1, mitochondrial	mitochondrial electron transport
Acaa2	Q8BWT1	3-ketoacyl-CoA thiolase, mitochondrial	fatty acid beta-oxidation
Aco2	Q99K10	Aconitate hydratase, mitochondrial	fatty acid beta-oxidation
Gpd2	AZAQR0	Glycerol-3-phosphate dehydrogenase	Tricarboxylic acid cycle
Sdhb	Q9CQA3	Succinate dehydrogenase [ubiquinone] iron-sulfur subunit, mitochondrial	glycerol-3-phosphate metabolic process
Ndufc2	Q9CQ54	NADH dehydrogenase [ubiquinone] 1 subunit C2	glycerol-3-phosphate metabolic process
Pcx	G5EBR3	Pyruvate carboxylase	mitochondrial electron transport chain, tricarboxylic acid cycle
Pcca	Q91ZA3	Propionyl-CoA carboxylase alpha chain, mitochondrial	mitochondrial electron transport
Ndufb4	Q9CQC7	NADH dehydrogenase [ubiquinone] 1 beta subcomplex subunit 4	pyruvate metabolic process
Pdha1	P35486	Pyruvate dehydrogenase E1 component subunit alpha, somatic form, mitochondrial	propanoyl-CoA degradation
Myh4	Q5SX39	Myosin-4	mitochondrial electron transport
Hspa8	Q504P4	Heat shock cognate 71 kDa protein	Tricarboxylic acid cycle
			Muscle contraction
			ATP binding

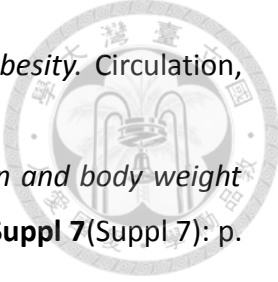


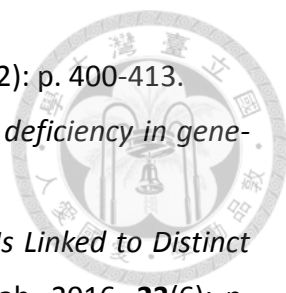
REFERENCE

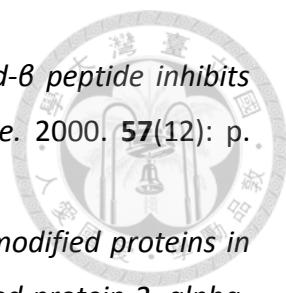
1. Yin, S.J., *Alcohol dehydrogenase: enzymology and metabolism*. Alcohol Alcohol Suppl, 1994. **2**: p. 113-9.
2. Eriksson, C.J., M. Marselos, and T. Koivula, *Role of cytosolic rat liver aldehyde dehydrogenase in the oxidation of acetaldehyde during ethanol metabolism in vivo*. Biochem J, 1975. **152**(3): p. 709-12.
3. Klyosov, A.A., et al., *Possible role of liver cytosolic and mitochondrial aldehyde dehydrogenases in acetaldehyde metabolism*. Biochemistry, 1996. **35**(14): p. 4445-56.
4. Yoval-Sanchez, B. and J.S. Rodriguez-Zavala, *Differences in susceptibility to inactivation of human aldehyde dehydrogenases by lipid peroxidation byproducts*. Chem Res Toxicol, 2012. **25**(3): p. 722-9.
5. Chen, C.H., et al., *Targeting aldehyde dehydrogenase 2: new therapeutic opportunities*. Physiol Rev, 2014. **94**(1): p. 1-34.
6. Enomoto, N., et al., *Acetaldehyde metabolism in different aldehyde dehydrogenase-2 genotypes*. Alcohol Clin Exp Res, 1991. **15**(1): p. 141-4.
7. Edenberg, H.J., *The genetics of alcohol metabolism: role of alcohol dehydrogenase and aldehyde dehydrogenase variants*. Alcohol Res Health, 2007. **30**(1): p. 5-13.
8. Larson, H.N., H. Weiner, and T.D. Hurley, *Disruption of the coenzyme binding site and dimer interface revealed in the crystal structure of mitochondrial aldehyde dehydrogenase "Asian" variant*. The Journal of biological chemistry, 2005. **280**(34): p. 30550-30556.
9. Perez-Miller, S., et al., *Alda-1 is an agonist and chemical chaperone for the common human aldehyde dehydrogenase 2 variant*. Nature Structural & Molecular Biology, 2010. **17**: p. 159.
10. Eriksson, C.J., *The role of acetaldehyde in the actions of alcohol (update 2000)*. Alcohol Clin Exp Res, 2001. **25**(5 Suppl ISBRA): p. 15S-32S.
11. Brooks, P.J., et al., *The alcohol flushing response: an unrecognized risk factor for esophageal cancer from alcohol consumption*. PLoS Med, 2009. **6**(3): p. e50.
12. Li, H., et al., *Refined geographic distribution of the oriental ALDH2*504Lys (nee 487Lys) variant*. Ann Hum Genet, 2009. **73**(Pt 3): p. 335-45.

- 
13. Vasiliou, V., A. Pappa, and T. Estey, *Role of Human Aldehyde Dehydrogenases in Endobiotic and Xenobiotic Metabolism*. *Drug Metabolism Reviews*, 2004. **36**(2): p. 279-299.
 14. Salaspuro, M., *Acetaldehyde as a common denominator and cumulative carcinogen in digestive tract cancers*. *Scandinavian Journal of Gastroenterology*, 2009. **44**(8): p. 912-925.
 15. O'Brien, P.J., A.G. Siraki, and N. Shangari, *Aldehyde sources, metabolism, molecular toxicity mechanisms, and possible effects on human health*. *Crit Rev Toxicol*, 2005. **35**(7): p. 609-62.
 16. LoPachin, R.M. and T. Gavin, *Molecular mechanisms of aldehyde toxicity: a chemical perspective*. *Chemical research in toxicology*, 2014. **27**(7): p. 1081-1091.
 17. Nelson, M.-A.M., S.P. Baba, and E.J. Anderson, *Biogenic Aldehydes as Therapeutic Targets for Cardiovascular Disease*. *Current opinion in pharmacology*, 2017. **33**: p. 56-63.
 18. Esterbauer, H., R.J. Schaur, and H. Zollner, *Chemistry and biochemistry of 4-hydroxynonenal, malonaldehyde and related aldehydes*. *Free Radic Biol Med*, 1991. **11**(1): p. 81-128.
 19. Zarkovic, K., *4-hydroxynonenal and neurodegenerative diseases*. *Mol Aspects Med*, 2003. **24**(4-5): p. 293-303.
 20. Zarkovic, N., *4-hydroxynonenal as a bioactive marker of pathophysiological processes*. *Mol Aspects Med*, 2003. **24**(4-5): p. 281-91.
 21. Frohnert, B.I. and D.A. Bernlohr, *Protein carbonylation, mitochondrial dysfunction, and insulin resistance*. *Adv Nutr*, 2013. **4**(2): p. 157-63.
 22. Marnett, L.J., J.N. Riggins, and J.D. West, *Endogenous generation of reactive oxidants and electrophiles and their reactions with DNA and protein*. *J Clin Invest*, 2003. **111**(5): p. 583-93.
 23. Calingasan, N.Y., K. Uchida, and G.E. Gibson, *Protein-bound acrolein: a novel marker of oxidative stress in Alzheimer's disease*. *J Neurochem*, 1999. **72**(2): p. 751-6.
 24. LoPachin, R.M., D.S. Barber, and T. Gavin, *Molecular mechanisms of the conjugated alpha,beta-unsaturated carbonyl derivatives: relevance to neurotoxicity and neurodegenerative diseases*. *Toxicol Sci*, 2008. **104**(2): p. 235-49.

- 
25. Choi, K. and Y.B. Kim, *Molecular mechanism of insulin resistance in obesity and type 2 diabetes*. Korean J Intern Med, 2010. **25**(2): p. 119-29.
 26. Furukawa, S., et al., *Increased oxidative stress in obesity and its impact on metabolic syndrome*. The Journal of clinical investigation, 2004. **114**(12): p. 1752-1761.
 27. Li, C., et al., *Aldehyde Dehydrogenase-2 Attenuates Myocardial Remodeling and Contractile Dysfunction Induced by a High-Fat Diet*. Cellular Physiology and Biochemistry, 2018. **48**(5): p. 1843-1853.
 28. Pillon, N.J. and C.O. Soulage, *Lipid peroxidation by-products and the metabolic syndrome, in Lipid Peroxidation*. 2012, IntechOpen.
 29. Uchida, K., et al., *Activation of stress signaling pathways by the end product of lipid peroxidation. 4-hydroxy-2-nonenal is a potential inducer of intracellular peroxide production*. J Biol Chem, 1999. **274**(4): p. 2234-42.
 30. Pillon, N.J., et al., *The lipid peroxidation by-product 4-hydroxy-2-nonenal (4-HNE) induces insulin resistance in skeletal muscle through both carbonyl and oxidative stress*. Endocrinology, 2012. **153**(5): p. 2099-111.
 31. Schauenstein, E., *Autoxidation of polyunsaturated esters in water: chemical structure and biological activity of the products*. J Lipid Res, 1967. **8**(5): p. 417-28.
 32. Singh, S.P., et al., *Role of the electrophilic lipid peroxidation product 4-hydroxynonenal in the development and maintenance of obesity in mice*. Biochemistry, 2008. **47**(12): p. 3900-11.
 33. Frohnert, B.I., et al., *Increased adipose protein carbonylation in human obesity*. 2011. **19**(9): p. 1735-1741.
 34. Miwa, I., et al., *Inhibition of glucose-induced insulin secretion by 4-hydroxy-2-nonenal and other lipid peroxidation products*. Endocrinology, 2000. **141**(8): p. 2767-72.
 35. Ihara, Y., et al., *Pancreatic (B-Cells of GK Rats, a Model of Type 2 Diabetes*. 1999. **48**.
 36. Shearn, C.T., et al., *Modification of Akt2 by 4-hydroxynonenal inhibits insulin-dependent Akt signaling in HepG2 cells*. Biochemistry, 2011. **50**(19): p. 3984-96.
 37. Demozay, D., et al., *FALDH Reverses the Deleterious Action of Oxidative Stress Induced by Lipid Peroxidation Product 4-Hydroxynonenal on Insulin Signaling in 3T3-L1 Adipocytes*. 2008. **57**(5): p. 1216-1226.

- 
38. Hill, J.O., H.R. Wyatt, and J.C. Peters, *Energy balance and obesity*. *Circulation*, 2012. **126**(1): p. 126-132.
39. Galgani, J. and E. Ravussin, *Energy metabolism, fuel selection and body weight regulation*. *International journal of obesity* (2005), 2008. **32 Suppl 7**(Suppl 7): p. S109-S119.
40. Cannon, B. and J. Nedergaard, *Brown adipose tissue: function and physiological significance*. *Physiol Rev*, 2004. **84**(1): p. 277-359.
41. Serra, D., et al., *Mitochondrial fatty acid oxidation in obesity*. *Antioxidants & redox signaling*, 2013. **19**(3): p. 269-284.
42. Calderon-Dominguez, M., et al., *Fatty acid metabolism and the basis of brown adipose tissue function*. *Adipocyte*, 2015. **5**(2): p. 98-118.
43. Feldmann, H.M., et al., *UCP1 ablation induces obesity and abolishes diet-induced thermogenesis in mice exempt from thermal stress by living at thermoneutrality*. *Cell Metab*, 2009. **9**(2): p. 203-9.
44. Ellis, J.M., et al., *Adipose acyl-CoA synthetase-1 directs fatty acids toward beta-oxidation and is required for cold thermogenesis*. *Cell metabolism*, 2010. **12**(1): p. 53-64.
45. Lee, J., J.M. Ellis, and M.J. Wolfgang, *Adipose fatty acid oxidation is required for thermogenesis and potentiates oxidative stress-induced inflammation*. *Cell reports*, 2015. **10**(2): p. 266-279.
46. Cypess, A.M., et al., *Identification and importance of brown adipose tissue in adult humans*. *The New England journal of medicine*, 2009. **360**(15): p. 1509-1517.
47. Luu, S.U., et al., *Ethanol and acetaldehyde metabolism in chinese with different aldehyde dehydrogenase-2 genotypes*. *Proc Natl Sci Counc Repub China B*, 1995. **19**(3): p. 129-36.
48. Wen, W., et al., *Meta-analysis of genome-wide association studies in East Asian-ancestry populations identifies four new loci for body mass index*. *Human molecular genetics*, 2014. **23**(20): p. 5492-5504.
49. Chang, Y.C., et al., *Common ALDH2 genetic variants predict development of hypertension in the SAPPHiRe prospective cohort: gene-environmental interaction with alcohol consumption*. *BMC Cardiovasc Disord*, 2012. **12**: p. 58.
50. Fedorenko, A., P.V. Lishko, and Y. Kirichok, *Mechanism of fatty-acid-dependent*

- 
- UCP1 uncoupling in brown fat mitochondria*. Cell, 2012. **151**(2): p. 400-413.
51. Tolwani, R.J., et al., *Medium-chain acyl-CoA dehydrogenase deficiency in gene-targeted mice*. PLoS genetics, 2005. **1**(2): p. e23-e23.
52. Chondronikola, M., et al., *Brown Adipose Tissue Activation Is Linked to Distinct Systemic Effects on Lipid Metabolism in Humans*. Cell Metab, 2016. **23**(6): p. 1200-1206.
53. Poli, G., F. Biasi, and G. Leonarduzzi, *4-Hydroxynonenal-protein adducts: A reliable biomarker of lipid oxidation in liver diseases*. Mol Aspects Med, 2008. **29**(1-2): p. 67-71.
54. Long, E.K., D.M. Olson, and D.A. Bernlohr, *High-fat diet induces changes in adipose tissue trans-4-oxo-2-nonenal and trans-4-hydroxy-2-nonenal levels in a depot-specific manner*. Free radical biology & medicine, 2013. **63**: p. 390-398.
55. Castro, J.P., et al., *4-Hydroxynonenal (HNE) modified proteins in metabolic diseases*. Free Radic Biol Med, 2017. **111**: p. 309-315.
56. Ruskovska, T. and D.A. Bernlohr, *Oxidative stress and protein carbonylation in adipose tissue - implications for insulin resistance and diabetes mellitus*. Journal of proteomics, 2013. **92**: p. 323-334.
57. Tseng, Y.-H., A.M. Cypess, and C.R. Kahn, *Cellular bioenergetics as a target for obesity therapy*. Nature Reviews Drug Discovery, 2010. **9**: p. 465.
58. Gonzalez-Hurtado, E., et al., *Fatty acid oxidation is required for active and quiescent brown adipose tissue maintenance and thermogenic programming*. Molecular metabolism, 2018. **7**: p. 45-56.
59. Bhat, A.H., et al., *Oxidative stress, mitochondrial dysfunction and neurodegenerative diseases; a mechanistic insight*. Biomed Pharmacother, 2015. **74**: p. 101-10.
60. Bhatti, J.S., G.K. Bhatti, and P.H. Reddy, *Mitochondrial dysfunction and oxidative stress in metabolic disorders - A step towards mitochondria based therapeutic strategies*. Biochim Biophys Acta Mol Basis Dis, 2017. **1863**(5): p. 1066-1077.
61. Zhao, Y., et al., *Redox proteomic identification of HNE-bound mitochondrial proteins in cardiac tissues reveals a systemic effect on energy metabolism after doxorubicin treatment*. Free Radic Biol Med, 2014. **72**: p. 55-65.
62. Poli, G., et al., *4-hydroxynonenal: a membrane lipid oxidation product of medicinal interest*. Med Res Rev, 2008. **28**(4): p. 569-631.

- 
63. Shringarpure, R., et al., *4-Hydroxynonenal-modified amyloid- β peptide inhibits the proteasome: possible importance in Alzheimer's disease*. 2000. **57**(12): p. 1802-1809.
64. Castegna, A., et al., *Proteomic identification of oxidatively modified proteins in Alzheimer's disease brain. Part II: dihydropyrimidinase-related protein 2, alpha-enolase and heat shock cognate 71*. J Neurochem, 2002. **82**(6): p. 1524-32.
65. Grune, T., et al., *Increased levels of 4-hydroxynonenal modified proteins in plasma of children with autoimmune diseases*. 1997. **23**(3): p. 357-360.
66. Naito, Y., et al., *Lipid hydroperoxide-derived modification of proteins in gastrointestinal tract*. Subcell Biochem, 2014. **77**: p. 137-48.
67. Nakamura, K., et al., *Carvedilol decreases elevated oxidative stress in human failing myocardium*. 2002. **105**(24): p. 2867-2871.
68. Biasi, F., et al., *Associated changes of lipid peroxidation and transforming growth factor β 1 levels in human colon cancer during tumour progression*. 2002. **50**(3): p. 361-367.
69. Marquez-Quiñones, A., et al., *HNE-protein adducts formation in different pre-carcinogenic stages of hepatitis in LEC rats*. 2010. **44**(2): p. 119-127.